Knee Surg Sports Traumatol Arthrosc (2013) 21:1151–1157
DOI 10.1007/s00167-012-2008-4

SHOULDER

Nonlinear stress analysis of the supraspinatus tendon using three-dimensional finite element analysis

Atsushi Inoue · Etsuo Chosa · Keisuke Goto · Naoya Tajima

Received: 8 August 2011 / Accepted: 12 April 2012 / Published online: 23 May 2012

Abstract
Purpose No studies have used stress analysis with finite element analysis (FEA) to determine the causes of and mechanisms underlying rotator cuff tears. Therefore, we performed a biomechanical evaluation of the changes in stress distribution on the rotator cuff using three-dimensional (3-D) FEA.
Methods The 3-D FEA model of shoulder joint allowed for abduction angles of 0°, 45° and 90° from the plane of the scapula and included the anatomical insertion points of the three major rotator cuff tendons and the middle fibres of the deltoid muscle. Stress distribution of the supraspinatus tendon on 3-D FEA was validated by a comparison with cadaveric and two-dimensional finite element model.
Results The principal stress peaked in the region approximately 1 cm proximal to the insertion of the supraspinatus tendon. Furthermore, the stress on the joint side increased at the anterior edge of the supraspinatus tendon at abduction angles of 45° and 90°.
Conclusion There are differences in stress changes between the joint side and bursal side of the supraspinatus tendon within the angles of abduction. The maximal tensile stress was observed on the articular side of the anterior edge of the supraspinatus tendon at 90° abduction. Our results indicate that the difference in tensile stress between the two layers results in delamination and causes partial-thickness tears.
Level of evidence Decision analysis, Level II.

Keywords Shoulder joint · Rotator cuff tear · Supraspinatus tendon · Abduction angle · Three-dimensional finite element analysis

A. Inoue (✉) · E. Chosa
Division of Orthopedic Surgery, Department of Medicine of Sensory and Motor Organs, Faculty of Medicine, University of Miyazaki, 5200 Kihara, Kiyotake, Miyazaki 889-1692, Japan
e-mail: ino619@yahoo.co.jp

A. Inoue · K. Goto · N. Tajima
Department of Orthopaedic Surgery, Nozaki Higashi Hospital, 2105 Takason, Murasumi, Miyazaki 880-0837, Japan

Introduction

Rotator cuff tear is a common pathological disorder of the shoulder. The mechanisms by which cuff tear size and location affect joint strength have not been well established. Although there are many epidemiological studies of rotator cuff tears, most mechanical analyses have involved the study of cadavers. Cadaveric studies reported that the difference in strain resulted between the superficial and deep layers of the supraspinatus tendon during abduction. [7, 15]. Cadaveric studies can be problematic with regard to muscles and tendons, because they are particularly affected by ageing and individual differences. Moreover, no studies have attempted to determine the causes or mechanisms of rotator cuff tears. Simulation by finite element analysis (FEA) allows us to perform mechanical investigations with conditions that are closer to those of the living body by developing an accurate model.

There are almost no stress analysis–based studies of the rotator cuff. Although a stress analysis of the supraspinatus tendon was performed using a simple model of a portion of the humerus and the supraspinatus muscle, it did not reflect the entire shoulder joint. Furthermore, the study analysed the tendon only at 0° abduction in the FEA model [17]. We have not been able to find any studies where a nonlinear analysis of the characteristics of the supraspinatus muscle

was performed using a model of the shoulder joint. Therefore, in this study, we created a three-dimensional (3-D) FEA model of a normal shoulder joint, which included the rotator cuff and the deltoid muscle. We then performed a nonlinear stress analysis of the supraspinatus muscle in each of the three angles of abduction (0°, 45°, 90°). The purpose of the present study was to investigate the mechanism and development of the rotator cuff tears with respect to the abduction angle and to the changes in stress on the supraspinatus muscle. We hypothesise that there are differences in stresses in the articular and bursal sides of the rotator cuff on increasing the abduction angle, causing shearing between the two layers resulting in delamination and partial-thickness tears.

Materials and methods

Shoulder joint modelling using FEA

The geometric data needed to create an FEA model were obtained from CT scanning (slice thickness, 2 mm) of the shoulder joint of a healthy 29-year-old male subject who gave informed consent and had no clinical or radiological abnormalities. Using these images, we developed an FEA model that allowed for abduction angles of 0°, 45° and 90° from the scapula plane. A cortical bone model was used, and the humerus was defined as hollow. The model also included the three major rotator cuff tendons (supraspinatus, infraspinatus and subscapularis tendons) and deltoid muscle [1, 14]. The external contour of the bone and soft tissue was defined on CT slice. The curves obtained were transferred and used to reconstruct the 3-D geometry of the shoulder joint. The tendons were assumed to be an isoparametric solid between the two insertions on the bone surfaces, wound around the reconstructed bone geometry.

The joint space observed in the CT scan images between the humerus and scapula was filled with cartilage. The minimum gap was measured, and the 3-D cartilage was reconstructed with a constant thickness equal to half this distance [3].

The geometric shape was composed of hexahedral meshes. The model had 58,245 nodes and 32,841 elements (Fig. 1). The material constants were obtained from the literature [17, 18]. For cortical bone, the Young's modulus was 1.5 GPa and the Poisson's ratio was 0.3. For the rotator cuff tendons and the deltoid muscle, we used the nonlinear stress–strain curve reported previously [5, 12] (Table 1). In the present study, only the passive behaviour of the tendons and muscle was accounted for. The passive stress–strain law was applied for other joint soft tissue such as ligaments and tendons.

The scapula was fixed on the *x*-, *y*-, and *z*-axes. The glenohumeral joint and the subacromial arch were each connected with a gap element. The coefficient of friction was predetermined as 0. The 3-D FEM analysis was performed using Solid Works' COSMOS Works 2006 software (Structural Research and Analysis Corporation, Los Angeles, CA, USA).

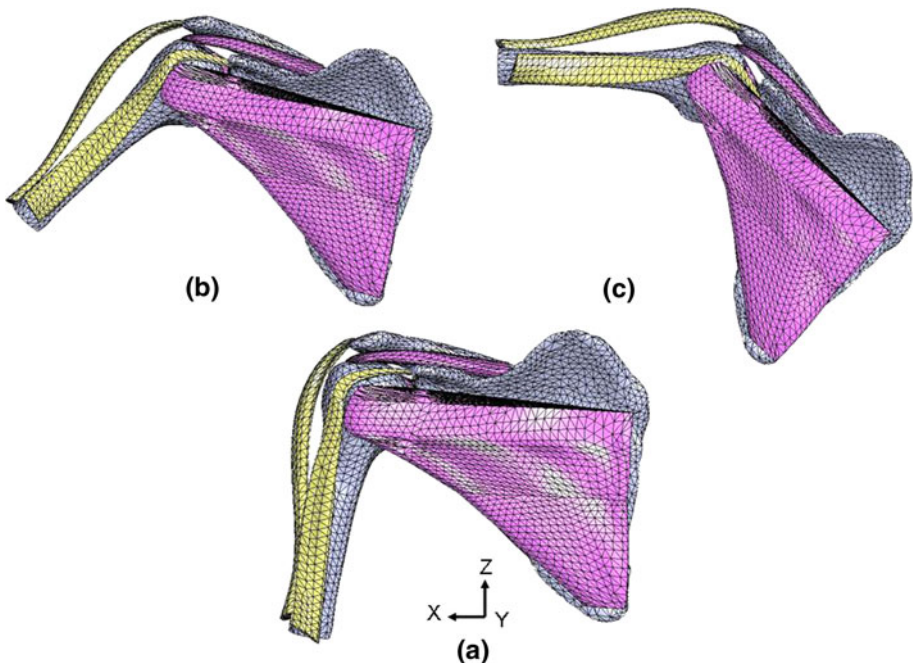

Fig. 1 3-D model of a normal shoulder joint. **a** 0° abduction. **b** 45° abduction. **c** 90° abduction

Table 1 Element types and material properties

Material	Element type	Young's modulus (MPa)	Poisson's ratio (v)
Cortical bone			
Humerus	Solid	15,000	0.3
Scapula	Solid	15,000	0.3
Articular cartilage	Solid	15	0.45
Muscle			
Supraspinatus	Solid	Nonlinear	
Infraspinatus	Solid	Nonlinear	
Subscapularis	Solid	Nonlinear	
Mid. deltoid	Solid	Nonlinear	
Articular surface	Contact	Frictionless	
Subacrominal space	Contact	Frictionless	

Nonlinear analysis of the supraspinatus tendon stress during abduction

With 0° abduction as the starting point, stress analyses were performed at 45° and 90° abduction while progressively increasing the loads and applying abduction to mimic dynamic motion within the limitations of static FEA. The loads were applied to the major abductor muscles, namely the middle fibres of the deltoid, as well as the rotator cuff (supraspinatus, infraspinatus and subscapularis) tendons. The loads on the tendon groups used in abduction were taken from the cadaveric study of previous reports [1, 8, 14]. Rotator cuff tendons were modeled as isolated three tendon bundles. Capsular ligaments were represented using 2-Node cables, for supraspinatus, subscapularis and infraspinatus tendon were connected as a function of the rotator cuff unit. The tensile load was applied to the proximal of the tendon in the direction of the long axis of supraspinatus tendon. Other cuff muscles were applied in the direction of distal muscle line. The deltoid muscle force was directed to the anterolateral corner of the acromion where the muscle has a board origin [1, 14]. For nonlinear analysis, force control was used as the numerical procedure, and the Newton–Raphson method was used as an iterative method, the load being applied in 10 steps by an incremental loading method. Mentioning about the computed program setting, the maximum equilibrium iterations in every step was 100 cycles. Errors in calculation were set up to 0.01. The force at each angle of abduction was determined from the theoretically predicted values [8]. For evaluation, the results of our analysis from the 3-D FEA model were then compared with those from a cadaveric study [15] and 2-D FEA model [21]. The reaction force on the glenoid fossa was measured to quantify the relationship between the rotator cuff and bone model at abduction. The von Mises stress on the glenoid was examined in these models.

The maximum principal stress within the supraspinatus tendon was calculated at each angle of abduction. Furthermore, the differences in stress changes between the bursal side (superficial layer) and the articular side (deep layer) of the supraspinatus tendon during abduction were verified.

Results

Reaction forces of the glenohumeral joint

For each of the three abduction angles of 0°, 45° and 90°, a load was applied to the rotator cuff group (supraspinatus, infraspinatus, subscapularis tendons) and the deltoid muscle. The reaction force on the glenoid fossa of the scapula during abduction was measured. The von Mises stress on the glenoid fossa of the scapula increased with an increase in the abduction angle.

Stress distribution in the supraspinatus tendon

The distribution of the principal stress in the supraspinatus tendon in each of the three abduction angles of 0°, 45° and 90° is shown in Table 2.

Upon insertion of the supraspinatus tendon, the maximal principal stress could be observed in all the FEA models. The principal stress on the supraspinatus tendon increased with the increase in the abduction angle. The principal stress peaked in the region approximately 10 mm proximal to the insertion of the supraspinatus tendon.

Differences between the bursal side and the articular side were analysed from the principal stresses. At 0° of abduction, no difference was observed in the principal stress between articular and bursal side of the supraspinatus tendon (Fig. 2). At 45° and 90° of abduction, the tensile stress on the articular side was higher than that on the bursal side. At 45° abduction, the stress was 7.6 times the average value at 0°. The maximum value was at the anterior portion of the articular surface, where

Table 2 Tensile stress related to the location of supraspinatus tendon

	Author portion	Middle portion	Posterior portion
Abduction 0°			
Articular side	1.1	0.5	0.2
Bursal side	0.5	0.5	0.9
Abduction 45°			
Articular side	11.9	2.0	1.9
Bursal side	4.0	6.6	1.4
Abduction 90°			
Articular side	15.9	9.6	7.6
Bursal side	5.4	9.1	7.1

Tensile stress is expressed in megapascals (MPa)

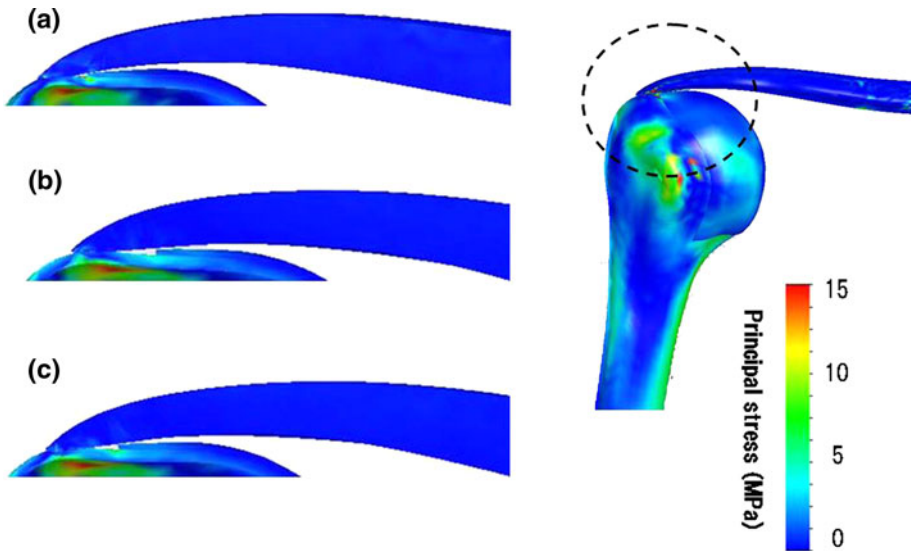

Fig. 2 Distributions of tensile stress in the supraspinatus tendon at 0° abduction. *Slice view* principal stress maximum in the sagittal plane through the **a** anterior, **b** middle, **c** posterior section of the supraspinatus tendon

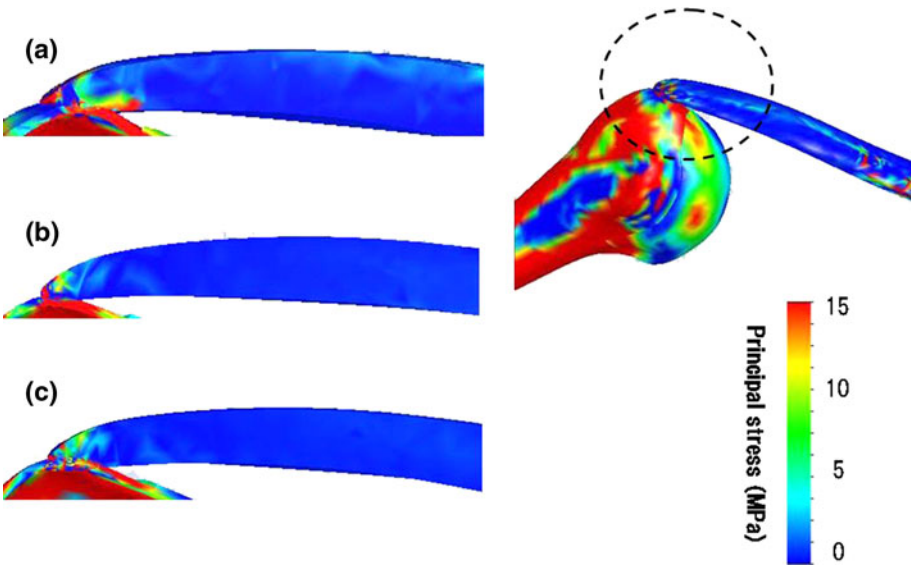

Fig. 3 Distributions of tensile stress in the supraspinatus tendon at 45° abduction. *Slice view* principal stress maximum in the sagittal plane through the **a** anterior, **b** middle, **c** posterior section of the supraspinatus tendon

it reached 11.9 MPa (Fig. 3). At 90° abduction, the stress was 14.9 times the average at 0°. The maximum value occurred on the anterior portion of the articular surface, where it reached 15.9 MPa (Fig. 4).

Discussion

The most important aspect of the present study was the investigation of nonlinear stress analysis of the supraspinatus tendon using 3-D FEA. As a result, we found the difference in stress in the articular and bursal sides of the rotator cuff on increasing abduction angle causes shearing between the two layers resulting in delamination, causing partial-thickness tears.

3-D versus 2-D finite element models

Modelling of the shoulder joint is difficult because of its complicated 3-D structure. The shoulder is a suspension joint composed of the upper humerus and the scapula. The scapula is mobile and has no fixed pivot point. Because it is supported by soft tissue, including the rotator cuff and the joint capsule, joint support is not stable. These factors make 3-D FEA complicated, and as a result, 2-D FEA has been used [11, 16, 21]. Moreover, 2-D FEA model were composed easily. 2-D FEA shows similar result with 3-D FEA in simple model. But in the complicated 3-D structure as shoulder joint, 3-D FEA performs better. Our result showed high concentration of tensile stress on the articular

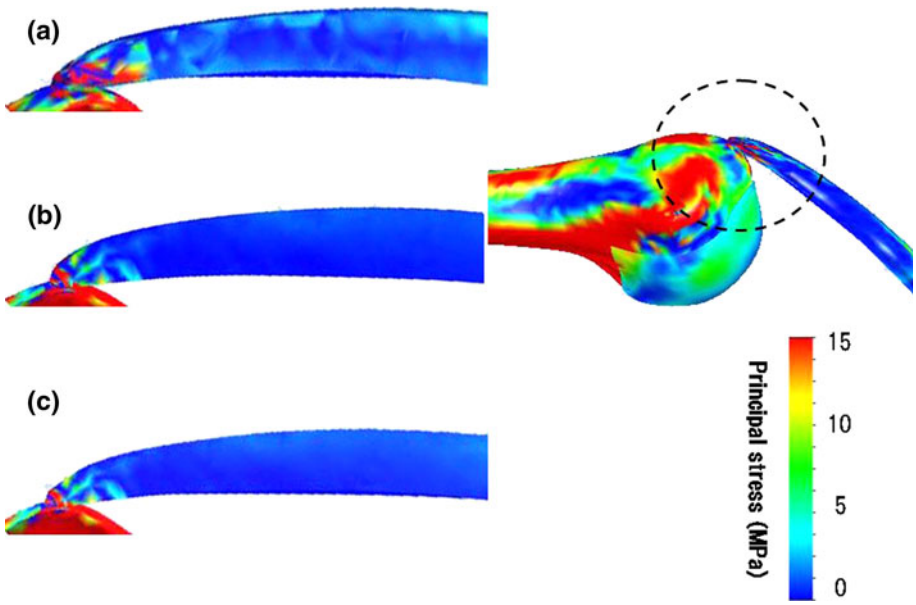

Fig. 4 Distributions of tensile stress in the supraspinatus tendon at 90° abduction. *Slice view* principal stress maximum in the sagittal plane through the **a** anterior, **b** middle, **c** posterior section of the supraspinatus tendon. The stress on the articular side was increased

side of the tendon. 2-D FEA studies showed maximum stress on the articular side in contact with the top of the humeral head. But their model does not have the antero-posterior dimension, so it is not clear which part of the supraspinatus tendon is in contact with the humeral head. 3-D FEA model was performed using the humeral head and the supraspinatus tendon, which reported stress concentrations at the point of attachment [17]. However, this is a simple model that does not reflect the entire shoulder joint. Rotator cuff is unit function, the model in humeral head and the supraspinatus tendon only is incomplete. Our model contains the rotator cuff tendons; each tendon combines the other tendons as the unit of rotator cuff. Compared with the other models, we created a shoulder joint FEA model with a structure that is close to that of the living body.

Evaluation with 3-D FEA model of shoulder joint in abduction

Reaction force of the glenohumeral joint

The rotator cuff muscles maintain glenohumeral stability by compressing the humeral head into the glenoid during active shoulder abduction. Reaction forces constitute an important aspect of shoulder biomechanics. Many reports predicted joint reaction forces to be 50 % of body weight and 330 N at 90° of abduction [6, 20]. The quantitative data obtained from the reaction force at the glenohumeral joint provided insight into the relationship between rotator cuff muscle force and joint motion. According to these data, the reaction forces at the glenohumeral joint reach 44 % of total body weight at maximum abduction [14]. In the model used in this analysis, the joint contact force was 336.5 N at 90° of abduction, which was 49 % body weight, which is comparable with the data reported in previous studies.

Stress distribution on supraspinatus tendon during shoulder abduction

Rotator cuff tears are well known to cause chronic pain and instability in the shoulder joint. The supraspinatus tendon surrounding the shoulder joint is a common site for rotator cuff tears. Such tears often occur in the portion of the supraspinatus tendon 1 cm proximal to the insertion in the humerus. This region was called the "critical zone" [4]. Structurally, this is where the synovial membrane, the joint capsule and tendon tissue join, causing it to be physiologically weak. Also, the region of 1-cm medial from the tendon insertion is an area of poor blood supply [9]. The cadaveric study reported that the supraspinatus tendon tears begin in the critical zone and increase in severity from there [7].

As a comparison was not made with cadavers, the validity of the model itself is questionable in some areas. This model was used to perform stress analyses at three angles of abduction: 0°, 45° and 90°.

Comparison with cadaveric data

Lindblom first reported that difference in the stresses in the articular and bursal sides of the rotator cuff causes shearing between the two layers, resulting in delamination and causing partial-thickness tears [10]. The articular and bursal sides of the rotator cuffs of 40 cadavers were

separated and tension applied to each layer [12]. It was found that the tears occurred as a result of histological differences: the bursal side is formed from a bundle of tendon fibres, whereas the articular side is formed from complex tissues consisting of tendon, ligament and capsular tissue, making it more susceptible to tears when put under tension. The tension experiments were performed on cadaveric humeri and supraspinatus muscles. They reported that, even with increasing abduction angles, the tension on the supraspinatus ligament on the articular side consistently increased more than that on the bursal side [15]. It is agreed that during abduction, irrespective of the layer, the strain is most influential, and the rupture spreads from there, resulting in the particulars of tear morphology. However, there is no consensus on the relationship between partial-thickness tears and full-thickness tears. It is accepted that there are differences in the composition of the articular and bursal side of the rotator cuff. Furthermore, the shear force between the two layers that arises from differences in stress can result in intratendinous tears, leading to full ruptures.

In contrast to mechanical studies of cadaveric shoulders, we used FEA to biomechanically evaluate the changes in stress distribution on the rotator cuff using 3-D FEA. In the results of our FEA, stress was also found to be concentrated in the anterior supraspinatus tendon proximal to the insertion point, in the location where rotator cuff tears commonly occur. We analysed the differences in tension between the bursal side and the articular side during abduction. The rotator cuff tension on the articular surface increased at 45° abduction; further, the tension increased at 90°. As described by Reilly et al. [15], our results show that abduction increased the supraspinatus tendon tension at the articular surface, leading to a tension difference between the two surfaces. However, there is biological difference because cadaveric model and clinical settings in this FEA model are varied, and our results should be interpreted with care.

Comparison with 2-D FEA model

Stress analysis of the supraspinatus tendon at shoulder abduction using 2-D FEA was reported [21]. High stress concentration was observed in the articular side of the supraspinatus tendon during arm elevation. In our 3-D FEA model, high stress concentration was observed in the articular side of the supraspinatus tendon during abduction. To analyze in the living shoulder more closely, we incorporated the acromion and other rotator cuff muscles into our model.

In reality, rotator cuff tears are not limited to this portion, and there are many forms of tears, which are categorized as bursal side, articular side and intratendinous tears. In throwing-injuries, articular surface tears are common, and as the abduction angle is increased, tears of the articular layer become more prevalent [22]. The morphology of rotator cuff tear was examined among one hundred and ten examples using magnetic resonance imaging and arthroscopy [19]. It was found that 75 % of tears at the 1–1.5 cm proximal to the tendon insertion point were articular side.

There are two mechanisms of rotator cuff tears. The intrinsic mechanism is that degenerative changes in the rotator cuff tendon result in tears. On the other hand, the extrinsic mechanism is that subacromial impingement results in rotator cuff tearing. There is a long-held idea that rotator cuff tears are caused by impact or abrasion at the point of insertion of the supraspinatus tendon, the so-called subacromial impingement [13]. It was proposed that 95 % of tears occur via this mechanism, and this idea has become widespread among orthopaedic surgeons in general. The stress was not only high in the acromial contact but remained at the magnitude throughout the tendon between articular and bursal boundaries with subacromial impingement. In this study, the high stress level was not observed in the area of supraspinatus tendon contacted with acromion. In normal 3-D FEA model, the coordinated function of the rotator cuff and deltoid muscles stabilizes the glenohumeral joint by compressing the humeral head into the glenoid. We will perform in the future that any imbalance in the functioning of the rotator cuff and deltoid muscles and various degrees of rotation during abduction affect the contact between tendon and acromion.

We have considered the morphology and the progression of rotator cuff tears in terms of the relationship between supraspinatus muscle strain and abduction angle. However, many other factors can be considered, including subacromial impingement due to acromial bone geometry, the condition of the rotator cuff with reduced muscle strength, and muscle balance of the rotator cuff group.

In the future, we plan to study degeneration due to age-related changes [2]. We will also consider changes in external forces applied to the rotator cuff, as well as investigate the mechanism of rotator cuff tearing through combined abduction-position conditions. Furthermore, validated FEA models can also be used to thoroughly investigate the effects of repeatedly applying varying loads.

The present study does not consider the effect of biological differences between individual subjects, activity, bone remodelling or the viscoelasticity of muscles and cartilage. There are some limitations concerning the FEA used in this study. We performed a nonlinear analysis of the tendon groups as isotropic material. There was no differentiation between muscles and tendons, or between the articular and bursal sides of the supraspinatus tendon. It is also necessary to keep in mind that soft tissues, such as

ligaments, the joint capsule and labrum, were not modelled in the present study, neither were joint pressure and scapular movement included. It should also be noted that kinetic and, therefore, dynamic analysis is not possible using FEA. The clinical usefulness of the present technique will be enhanced by considering the results of the present study together with those of the previous studies using cadavers, and keeping the above-mentioned limitations in mind.

This study is the first application of 3-D FEA of the rotator cuff in the abduction of shoulder joint. The results of this study have important relations for understanding shoulder strength in cuff tear and surgery, rehabilitation to treat cuff dysfunction. This model can be useful to investigate the effect of cuff tear size and tear location.

Conclusion

The aim of this 3-D FEA–based study was to investigate the relationship between supraspinatus tendon strain and abduction angles of shoulder joint. The maximal tensile stress was observed on the articular side of the anterior edge of the supraspinatus tendon at 90° abduction. We found differences in stress in the articular and bursal sides of the rotator cuff on increasing abduction angle cause shearing between the two layers resulting in delamination and causing partial-thickness tears.

Acknowledgments The authors thank the technicians at the Institute of Mechanical Systems Engineering and the Industrial Technology Center of Miyazaki for their valuable collaboration. This study was supported by a Grant-in-Aid from the Ministry of Education, Culture, Sports, Science and Technology of Japan. No financial remuneration related to the subject of this article was received by the authors or by any member of their families.

References

1. Apreleva M, Parsons IM, Warner JJP, Fu FH, Woo SLY (2000) Experimental investigation of reaction forces at the glenohumeral joint during active abduction. J Should Elbow Surg 9:409–417
2. Brewer BJ (1979) Aging of the rotator cuff. Am J Sports Med 7:102–110
3. Buchler B, Ramaniraka NA, Rakotomanaa LR, Ianotii JP, Farron A (2002) A finite element model of the shoulder: application to the comparison of ormal and osteoartritic joint. Clin Biomech 17:630–639
4. Codman EA (1931) The pathology associated with rupture of the supraspinatus tendon. Ann Surg 93:348–359
5. Goto K, Tajima N, Chosa E, Totoribe K, Kuroki H, Arizumi Y, Takashi A (2002) Mechanical analysis of the lumbar vertebrae in a three-dimensional finite element method model in which intradiscal pressure in the nucleus pulposus was used to establish the model. J Orthop Sci 7:243–246
6. Inman VT, Saunders M, Abbott LC (1944) Observations on the function of the shoulder joint. J Bone Jt Surg Am 42:1–30
7. Itoi E, Berblund LJ, Grabowski JJ, Schultz FM, Growney ES, Morrey BF, An KN (2005) Tensile properties of the supraspinatus tendon. J Orthop Res 13:578–584
8. Karlsson D, Peterson B (1992) Towards a model for force predictions in the human shoulder. J Biomech 25:189–199
9. Keyes EL (1935) Anatomical observations on senile changes in the shoulder. J Bone Jt Surg 17-A:953–960
10. Lindblom K (1939) On pathogenesis of ruptures of the tendon aponeurosis of the shoulder joint. Acta Radial 20:563–577
11. Luo ZP, Hsh HC, Grabowski JJ, Morrey BF, An KN (1998) Mechanical environment associated with rotator cuff tears. J Should Elbow Surg 7:616–620
12. Nakajima T, Rokuuma N, Hamada K, Tomatsu T, Fukuda H (1994) Histologic and biomechanical characteristics of the supraspinatus tendon: reference to rotator cuff tearing. J Should Elbow Surg 3:79–87
13. Neer CS (1983) Impingement lesions. Clin Orthop 173:70–77
14. Parsons IM, Apreleva M, Fu FH, Woo SLY (2002) The effect of the rotator cuff tears on reaction forces at the glenohumeral joint. J Orthop Res 20:439–446
15. Reilly P, Amis AA, Wallace AL, Emery RJH (2003) Mechanical factors in the initiation and propagation of tears the rotator cuff. J Bone Jt Surg 4:559–594
16. Sano H, Wakabayashi I, Itoi E (2006) Stress distribution in the supraspinatus tendon with partial thickness tears. J Should Elbow Surg 15:100–105
17. Seki N, Itoi E, Shibuya Y, Wakabayashi I, Sano H, Sashi R (2008) Mechanical environment of the supraspinatus tendon three-dimensional finite element model analysis. J Orthop Sci 13:348–353
18. Terrier A, Reist A, Vogel A, Farron A (2007) Effect of supraspinatus deficiency on humerus translation and glenohumeral contact force during abduction. Clin Biomech 22:645–651
19. Tuite MJ, Turnbull JR, Orwin JF (1998) Anterior versus posterior and rim-rent rotator cuff tears. Skeletal Radiol 27:237–243
20. Van der Helm FCT (1994) A finite element musculoskeletal model of the shoulder mechanism. J Biomech 24:551–569
21. Wakabayashi I, Itoi E, Sano H, Shibuya Y, Sashi R, Minagawa H, Kobayashi M (2003) Mechanical environment of the supraspinatus tendon: a two-dimensional finite element model analysis. J Should Elbow Surg 12:612–617
22. Walch G, Boileau P, Noel E, Donell ST (1992) Impingement of the deep surface of the supraspinatus tendon on the posterosuperior glenoid rim: an arthroscopic study. J Should Elbow Surg 1:238–245